



Sudan University of Science and Technology

College of graduate Studies



**Evaluation of Diffusely High Uptake of the Skull in Breast and Prostate  
Cancer using Bone Scintigraphy**

تقويم ارتفاع امتصاص الجمجمة في مسح العظام لمرضي سرطان الثدي والبروستاتا

*A Thesis Submitted for Partial Fulfillment for Requirements of Master Degree in  
Nuclear Medicine*

*By:*

Eshtiaq Abdelmoneim Ali Abd Alla

*Supervisor:*

*Dr. Eltayeb Wagiallah EltayebWagiallah*

2019

بسم الله الرحمن الرحيم

قال تعالى: (أَوْ كَالَّذِي مَرَّ عَلَى قَرْيَةٍ وَهِيَ خَاوِيَةٌ عَلَى عُرُوشِهَا قَالَ أَنَّى يُحْيِي هَذِهِ اللَّهُ بَعْدَ مَوْتِهَا ۗ فَأَمَاتَهُ اللَّهُ مِائَةَ عَامٍ ثُمَّ بَعَثَهُ ۗ قَالَ كَمْ لَبِثْتَ ۗ قَالَ لَبِثْتُ يَوْمًا أَوْ بَعْضَ يَوْمٍ ۗ قَالَ بَلْ لَبِثْتَ مِائَةَ عَامٍ فَانظُرْ إِلَى طَعَامِكَ وَشَرَابِكَ لَمْ يَتَسَنَّه ۗ وَانظُرْ إِلَى حِمَارِكَ وَلِنَجْعَلَ آيَةً لِلنَّاسِ ۗ وَانظُرْ إِلَى الْعِظَامِ كَيْفَ نُنشِزُهَا ثُمَّ نَكْسُوهَا لَحْمًا ۗ فَلَمَّا تَبَيَّنَ لَهُ قَالَ أَعْلَمُ أَنَّ اللَّهَ عَلَى كُلِّ شَيْءٍ قَدِيرٌ ﴿٢٥٩﴾)

صدق الله العظيم

## **Dedication**

*I dedicate my research to my Father who support me and drove me to where I am now. My Mother's soul who wish to see my success. To my family, and friends for their immense support and guidance.*

## Acknowledgement

*I would like to express my sincere gratitude to Associate Professor of Nuclear Medicine **Dr. Eltayeb WagiallahEltayeb** who has giving me great advise and help in the whole process of my thesis, for his fruitful day to day supervision, guidance, endless help and encouragement that built confidence in my work, for his continuous help, his patience, and for endless encouragement and unlimited support.*

*My thanks to my colleagues in Radiation and Isotopes Center of Khartoum (RICK), Nuclear Medicine Department for contributing in the sample collections. My friends for their immense support and guidance.*

*I would like to thank everyone who assisted by one way or another to bring this study to light.*

## **Abstract**

The National Cancer Registry in Sudan in (2016) found that the most common diagnosed cancer for the last ten years among women was breast cancer, and for men was Prostate cancer. Bone scan is a very important diagnostic and follow-up procedure for those patients, deciding the ideal treatment plan.

When reporting bone scans, it is important to distinguish between normal appearances and skeletal pathology; (cancer metastases), involving the skull. The limitations of WB scan reports at NM-departments in Khartoum state come because it depends on subjective reporting only, whereas in these cases the metastases occurred at a very sensitive part of human body and it's hard to distinguish for the most of the cases.

The general aim of this study is to evaluate a diffusely high uptake of skull in breast and prostate cancer using bone Scintigraphy. The study was done at Khartoum Oncology Hospital, for total of (100) adult patients of breast and prostate cancer with normal bone scans, and the data collected using master data collection sheet, and image were processing for the calculation of Skull uptake.

The main results of this study were: skull uptake showed significantly higher in female patients in the age groups (30-39 years and above). While in males the upper age groups (60-69 years and above) had significantly higher uptake than the lower age group. There was significant correlation between skull uptake and age ( $P<.001$ ) as well as with gender ( $P<.001$ ); (35 of female patients had higher uptake levels compare to 11 male patients).

This study concluded that “hot skull” is not necessarily an abnormal finding, especially in elderly women. Recommend that every nuclear medicine department

Considering the normal variants that can affect the reporting of bone scan, and uses its own normal values and reference samples for quantitative evaluation, due to racial or socio-economical variations.

## المستخلص

في العام 2016 وجد السجل القومي للسرطان أن سرطان الثدي هو الأكثر انتشارا عند النساء, وسرطان البروستاتا هو الأكثر انتشارا عند الرجال. يعتبر فحص مسح العظام ضروريا لتشخيص ومتابعة حالات المرضى وتحديد خطة العلاج المناسبة.

تقارير المسح الاشعاعي للعظام بأقسام الطب النووي في ولاية الخرطوم تعتمد بشكل عام علي النظرة الشخصية للطبيب فقط, لذلك عند كتابة تقرير فحص مسح العظام من الضروري التمييز بين التغييرات الطبيعية والمرضية التي قد تؤثر علي العظام(انتشار السرطان في العظام). كما أن سرطان الثدي والبروستاتا لديه قابلية عالية للانتشار في الدماغ لذلك لابد من التركيز علي منطقة الجمجمة أثناء الفحص.

الهدف العام من هذه الدراسة تقييم ارتفاع امتصاص الجمجمة في مسح العظام لمرضى سرطان الثدي والبروستاتا. أجريت الدراسة بمستشفى الخرطوم للأورام لعدد(100) مريض بالغ لا يعانون من انتشار للمرض في العظام, باستخدام ورقة جمع البيانات , ومن ثم أجريت معالجة للصور بغرض حساب نسبة امتصاص الجمجمة.

اثبتت نتائج هذه الدراسة ان الاناث من ابتداءا من عمر(30 سنة) وأعلي لديهن نسبة امتصاص أعلي, بينما عند الذكور يكون ارتفاع الامتصاص ابتداءا من عمر (60 سنة) مقارنة بالفئات العمرية الصغري. كما وجد أنه هنالك علاقة وثيقة بين امتصاص الجمجمة مع العمر والنوع ( $P < 0.001$ ).

أستخلصت الدراسة أن ارتفاع الامتصاص ليس من الضروري ان يكون علامة غير طبيعیه خاصة عند الفئات العمرية الكبرى لدي الاناث. كما أوصت بضرورة الأخذ في الاعتبار التغييرات الطبيعية التي من الممكن ان تؤثر علي امتصاص الجمجمة في مسح العظام, ووجهت كل أقسام الطب النووي بأن تضع قيم مرجعية لتقييم نسبة امتصاص الجمجمة الطبيعي للمواد المشعة مع مراعاة التغييرات الاقتصادية والاجتماعية والعرقية التي تختلف من مكان الي اخر.

## List of Contents

Subject	Page
الآية	I
Dedication	II
Acknowledgement	III
Abstract(English)	IV
Abstract(Arabic)	VI
List of tables	VII
List of figures	VIII
List of abbreviations	IX
<b>Chapter One</b>	
1.1 Introduction	1
1.2 problem statement	2
1.3 Objectives	3
1.4 significance of study	3
1.5 Overview of study	3
<b>Chapter Two</b>	
2.1 Anatomy and Physiology	4
2.1.1 Neurocranium	4
2.1.1.1 Occipital Bone	5
2.1.1.2 Temporal Bones	5
2.1.1.3 Parietal Bone	6
2.1.1.4 Sphenoid Bone	6
2.1.1.5 Ethmoid Bone	7
2.1.1.6 Frontal Bone	7
2.1.2 Viserocranium	7
2.1.2.1 Zygomatic Bones	8
2.1.2.2 Lacrimal Bones	8
2.1.2.3 Nasal Bones	8
2.1.2.4 Maxilla Bones	9
2.1.2.5 Palatine Bones	9
2.1.2.6 The Mandible	9
2.1.2.7 Orbits	9
2.1.2.8 Foramina	10
2.1.2.9 Sutures	11
2.1.2.10 Paranasal Sinsus	12
2.1.2.10.1 Functions of paranasal sinsus	13
2.2 Skull Metastasis	14

2.2.1 Epidemiology	14
2.2.2 Clinical Presentation	14
2.2.3 Pathology	14
2.2.4 Radiographic Features	15
2.2.5 Treatment	15
2.2.5.1 Radiotherapy	15
2.2.5.2 Chemotherapy	16
2.2.5.3 Surgery	16
2.2.6 Bone Scan	16
2.2.7 Diagnosis	18
2.2.8 Types of Bone Scan	18
2.2.8.1 Dynamic bone scans	18
2.2.8.1.1 Indications	18
2.2.8.2 Static Bone Scan:	19
2.2.8.2.1 Indications	19
2.2.8.2.2 Contraindication	19
2.2.9 Indications for Bone SPECT	19
2.2.10 Normal Scan	19
2.2.11 Abnormal Scan	21
2.3 Instrumentation for Radiation Detection and Measurement	22
2.3.1 Gas Filled Detector	22
2.3.2 Scintillation Detector Instrument	23
2.3.2.1 Collimator	24
2.3.2.2 Photocathode	25
2.3.2.3 Photomultiplier Tube	25
2.3.2.4 Preamplifier	25
2.3.2.5 Linear Amplifier	26
2.3.2.6 Pulse Height Analyzer	26
2.3.2.7 Display or Storage	27
2.4 Single Photon Emission Computed Tomography	27
2.5 Literature Review	28
<b>Chapter Three</b>	
3.1 Material	31
3.1.1 SPECT Camera	31
3.1.2 Procedure	31
3.2 Method	32
3.2.1 Study Design	32
3.2.2 Area of Study	32



3.2.3 Duration of Study	32
3.2.4 Population of study	32
3.2.5 Sample Size	33
3.2.6 Ethical Consideration	33
3.2.7 Data analysis and Presentation	33
Chapter Four	
4.1 Results	34
Chapter Five	
5.1 Discussion	39
5.2 Conclusion	40
5.3 Recommendations	41
References	42
Appendices	45

## List of Tables

Table No	Table Content	Page
4.1	frequency of patients according to age groups	34
4.2	frequency of skull uptake Vs body mass index	35
4.3	Cross tabulation of gender and age groups	36
4.4	Correlation between skull uptake and gender	37
4.5	Correlation between age groups and average uptake	38
4.6	frequency of skull uptake according to the disease	38

## List of Figures

Figure No	Figure Content	Page
2.1	Components of neurocranium	5
2.2	Components of Viscerocranium	8
2.3	Foramina of Skull	10
2.4	Lateral view of skull showing sutures	12
2.5	Sinuses	12
2.6	Normal Bone Scan	20
2.7	Normal Adult Bone Scan	20
2.8	Abnormal Bone Scan	21
2.9	A widespread skeletal metastasis	22
2.10	Schematic diagram of gas filled detector	23
2.11	Schematic diagram of Scintillation detector	24
2.12	Different types of collimators	24
2.13	SPECT Camera	28
3.1	SPECT Camera used in this Thesis	31
3.2	Example of ROI drawing on the skull	32
4.1	Distribution of patients according to the gender	34
4.2	Frequency of normal skull uptake in different BMI	35
4.3	Frequency of abnormal skull uptake in different BMI	36
4.4	Relationship between abnormal skull uptake among gender and age groups	37

## List of Abbreviations

BMI	Body Mass Index
Ca	Cancer
mCi	Millie Curie
NCR	National Cancer Registry
RICK	Radiation and Isotope Center of Khartoum
ROI	Region Of Interest
SPECT	Single Photon Computed Tomography

# Chapter One

## 1.1 Introduction

Bone scintigraphy is frequently performed to investigate many skeletal abnormalities (such as primary tumoural and metastatic involvement of the skeleton, infections of the bone and soft tissue, fractures and other traumatic lesions of the skeleton, etc.) in daily nuclear medicine practice. Age-related changes shown by whole-body bone scintigraphy with <sup>99m</sup>Tc-labeled phosphonates are well known, such as in growth plates, the sternum, and increased uptake diffusely in the skulls of postmenopausal women (Kakhki and Zakavi 2006)(Kigami, Yamamoto et al. 1996). A diffuse increased uptake in the calvarium (a “hot skull”) was first attributed to extensive cytotoxic treatment in patients with breast cancer, but studies that are more recent have shown this to be specific neither to breast cancer nor cytotoxic treatment (Kigami, Yamamoto et al. 1996). Metabolic disorders such as hyperparathyroidism and osteomalacia, as well as administration of chemotherapeutic drugs, can also cause increased skull uptake(Ryan and Fogelman 1997)(Pour, Simon-Corat et al. 2004).

The first National Population-based Cancer Registry (NCR) in Sudan found that the most commonly diagnosed cancer among women was breast followed by leukemia, cervix, and ovary, and among men it was prostate cancer followed by leukemia, lymphoma, oral, colorectal, and liver(Saeed, Weng et al. 2014).

A skull metastasis incidence rate 23% in patients with breast , lung or prostate cancer who underwent radionuclide bone scanning and the skull may be the only site of bony metastasis in up to(11.6%) of patients (Lam, de Klerk et al. 2007).

Radioisotope skull images of patients with benign and malignant neoplastic processes, trauma, Paget's disease and drug related increased tracer uptake will be shown. The rationale for using phosphonate compounds for bone scanning lies in the composition of the bone matrix containing calcium phosphate that can be exchanged with phosphonate compounds. Two compounds,  $^{99m}\text{Tc}$ -MDP and  $^{99m}\text{Tc}$ -HDP, are commercially available for bone imaging, of which  $^{99m}\text{Tc}$ -MDP. Approximately 10–20 mCi (370–740 MBq)  $^{99m}\text{Tc}$ -MDP or  $^{99m}\text{Tc}$ -HDP is injected intravenously and scanning is performed with the patient supine 2–3 h after injection (Saha 2012).

The most commonly seen patterns of abnormally increased uptake in the skull are solitary foci which cause doughnut appearance of radiotracer accumulation, patient with bone metastasis and metabolic diseases. Metastatic disease to the intracranial dura, the calvarium, and the skull base is relatively uncommon but presents unique diagnostic and management challenges in the patient with cancer. Modern imaging techniques have facilitated the detection of intracranial tumor deposits, leading to increased incidence. While dural and calvarial metastases often present with nonspecific symptoms, skull base metastases present with distinct clinical syndromes dependent on the local neurovascular structures affected (Lam, de Klerk et al. 2007).

## **1.2 Problem Statement:**

When reporting bone scans, it is important to distinguish between normal appearances and skeletal pathology; (cancer metastases), involving the skull. The limitations of WB scan reports at NM-departments in Khartoum state come because it depends on subjective reporting only, whereas in these cases the metastases occurred at a very sensitive part of human body and it's hard to distinguish for the most of the cases.

## **1.3 Objectives:**

### **1.3.1 General Objective:**

- To evaluate the diffusely high uptake by the skull in bone Scintigraphy.

### **1.3.2 Specific Objectives:**

- To compare between the different skulls uptake in the most presented cancers in Khartoum state.
- To find out the normal skull uptake level as an objective method for diagnosis of bone Scintigraphy.
- To characterize skull uptake according to age and gender.
- To correlate between skull uptake and body weight.

## **1.4 Significance of study:**

This study is an attempt to evaluate diffusely high uptake of skull using bone Scintigraphy to relate that to gender and age, as well as to predict the effect of body mass index on skull uptake.

## **1.5 Overview of study:**

This study was concerned with evaluation of diffusely high uptake of skull in bone Scintigraphy, this study will fall in five chapters : chapter one deal with the introduction, it represent statement of the study problems, objectives of the study, where chapter two coati the background material of the thesis especially it discusses the way of calculations used and different materials and method used, where chapter four presents the results and five deal with discussion ,conclusion and recommendations.

## **Chapter Two**

### **Literature Review Background and**

#### **2.1 Anatomy and Physiology of Skull:**

The skull supports the musculature and structures of the face and forms a protective cavity for the brain. The skull is formed of several bones which, with the exception of the mandible, are joined together by sutures—synarthrodial (immovable) joints (Bontrager and Lampignano 2013).

The human skull is the part of the skeleton that supports the structures of the face and forms a cavity for the brain. The adult human skull is comprised of twenty-two bones which are divided into two parts of differing embryological origin: the neurocranium and the viscerocranium (Bontrager and Lampignano 2013).

#### **2.1.1 Neurocranium**

The neurocranium forms the cranial cavity that surrounds and protects the brain and brainstem. The neurocranium is formed from the occipital bone, two temporal bones, two parietal bones, the sphenoid, ethmoid and frontal bones; they are all joined together with sutures (Bontrager and Lampignano 2013).



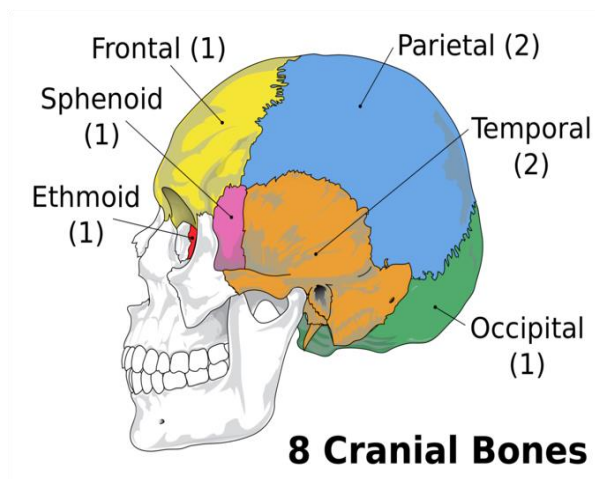


**Figure 2.1** Shows Components of neurocranium (Bontrager and Lampignano 2013).

### **2.1.1.1 Occipital Bone**

The occipital bone forms the base of the skull at the rear of the cranium. It articulates with the first vertebra of the spinal cord and also contains the foramen magnum, the large opening of the skull through which the spinal cord passes as it enters the vertebral column. The occipital bone borders the parietal bones through the heavily serrated lambdoidal suture, and also the temporal bones through occipitomastoid suture (Bontrager and Lampignano 2013).

### **2.1.1.2 Temporal Bones**

The temporal bones are situated at the base and sides of the skull, lateral to the temporal lobes of the brain. The temporal bones consist of four regions the squamous, mastoid, petrous and tympanic regions. The squamous region is the largest and most superior region. Inferior to the squamous is the mastoid region, and fused between the squamous and mastoid regions is the petrous region. Finally, the small and inferior

tympanic region lies anteriorly to the mastoid(Bontrager and Lampignano 2013).

### **2.1.1.3 Parietal Bones:**

The two large parietal bones are connected and make up part of the roof and sides of the human skull. The two bones articulate to form the sagittal suture. In the front, the parietal bones form the coronal suture with the frontal bone, and in the rear, the lambdoid suture is formed by the occipital bone. Finally, the squamosal suture separates the parietal and temporal bones(Bontrager and Lampignano 2013).

### **2.1.1.4 Sphenoid Bone**

The sphenoid bone is situated in the middle of the skull towards the front and forms the rear of the orbit. It has been described as resembling a butterfly due to its wing-like processes. The sphenoid bone is divided into several parts: the body of the bone, two greater wings, two lesser wings, and the pterygoid processes(Bontrager and Lampignano 2013).

The sphenoid bone is one of the most complexes in the body due to its interactions with numerous facial bones, ligaments, and muscles. The body that forms the middle of the sphenoid bone articulates with the ethmoid and occipital bone and forms a key part of the nasal cavity; it also contains the sphenoidal sinuses(Bontrager and Lampignano 2013).

The greater wings form the floor of the middle cranial fossa that houses the frontal lobes and pituitary gland, and also the posterior wall of the orbit. The lesser wings project laterally and form the floor of the anterior cranial fossa and the superior orbital fissure through which several key optical nerves pass(Bontrager and Lampignano 2013).

### **2.1.1.5 Ethmoid Bone**

The ethmoid bone is a small bone in the skull that separates the nasal cavity from the brain. It is lightweight due to its spongy, air-filled construction and is located at the roof of the nose and between the two orbits.

The ethmoid bone forms the medial wall of the orbit, the roof of the nasal cavity, and due to its central location it articulates with numerous bones of the viscerocranium. Inside the neurocranium it articulates with the frontal and sphenoid bones(Bontrager and Lampignano 2013).

### **2.1.1.6 Frontal Bone**

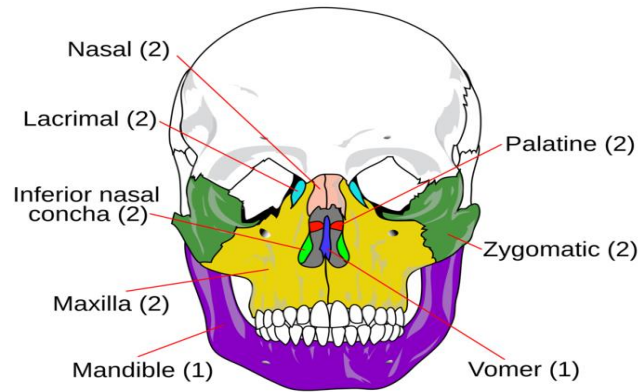
The frontal bone forms the front of the skull and is divided into three parts:Squamous(This part is large and flat and forms the main region of the forehead), Orbital (This part lies inferiorly and forms the superior border of the orbit) and Nasal (This part is smaller and articulates with the nasal bones and maxilla to contribute to the roof of the nose).

The frontal bone borders two other neurocranial bones—the parietal bones through the coronal sutures and the sphenoid bone through the sphenofrontal suture. It also articulates with the zygomatic and nasal bones and the maxilla(Bontrager and Lampignano 2013).

## **2.1.2 Viscerocranium**

The viscerocranium or facial bones support the soft tissue of the face. The viscerocranium consists of 14 individual bones that fuse together.

However, the hyoid bone, ethmoid bone, and sphenoid bones are sometimes included in the viscerocranium(Bontrager and Lampignano 2013).



### **14 Facial Bones**

**Figure 2.2** Shows Components of viscerocranium (Bontrager and Lampignano 2013).

#### **2.1.2.1 Zygomatic Bones**

The two zygomatic bones form the cheeks and contribute to the orbits. They articulate with the frontal, temporal, maxilla, and sphenoid bones (Bontrager and Lampignano 2013).

#### **2.1.2.2 Lacrimal Bones**

The two lacrimal bones form the medial wall of the orbit and articulate with the frontal, ethmoid, maxilla, and inferior nasal conchae. The lacrimal bones are the two smallest bones located in the face (Bontrager and Lampignano 2013).

#### **2.1.2.3 Nasal Bones**

The two slender nasal bones located in the midline of the face fuse to form the bridge of the nose and also articulate with the frontal, ethmoid and maxilla bones. The inferior nasal conchae are located within the nasal cavity. They are spongy and curled in shape; their primary function is to increase the surface area of the nasal cavity, which also increases the

amount of air that contacts the mucous membranes and cilia of the nose, thus filtering, warming, and humidifying the air before it enters the lungs. At the base of the nasal cavity is the small vomer bone which forms the nasal septum(Bontrager and Lampignano 2013).

#### **2.1.2.4 Maxilla Bones**

The maxilla bones fuse in the midline and form the upper jaw. They provide the bed for the upper teeth, the floor of the nose, and the base of the orbits. The maxilla articulates with the zygomatic, nasal, lacrimal, and palatine bones(Bontrager and Lampignano 2013).

#### **2.1.2.5 Palatine Bones**

The palatine bones fuse in the midline to form the palatine, located at the back of the nasal cavity that forms the roof of the mouth and the floor of the orbit(Bontrager and Lampignano 2013).

#### **2.1.2.6 The Mandible**

Finally, the mandible forms the lower jaw of the skull. The joint between the mandible and the temporal bones of the neurocranium, known as the temporo mandibular joint, forms the only non-sutured joint in the skull(Bontrager and Lampignano 2013).

#### **2.1.2.7 Orbits**

The orbit is the cavity or socket of the skull in which the eye and its appendages are situated.

The orbit, or eye socket, is the cavity located in the skull in which the eye and its associated appendages are housed. The orbits are conical, sometimes described as four-sided pyramidal, cavities that open in the

midline of the face and point backwards. To the rear of the orbit, the optic foramen opens into the optical canal through which the optic nerve and ophthalmic artery pass(Bontrager and Lampignano 2013).

The primary functions of the orbit include protection of its delicate contents and, through muscle attachment and a smooth coating fascia, to also promote the smooth, delicate movements of the eye(Bontrager and Lampignano 2013).

### 2.1.2.8 Foramina

The human skull has numerous holes known as foramina through which cranial nerves. The human skull has numerous foramina through which cranial nerves, arteries, veins, and other structures pass. The skull bones that contain foramina include the frontal, ethmoid, sphenoid; maxilla, palatine, temporal, and occipital lobes, arteries, veins, and other structures pass(Bontrager and Lampignano 2013).

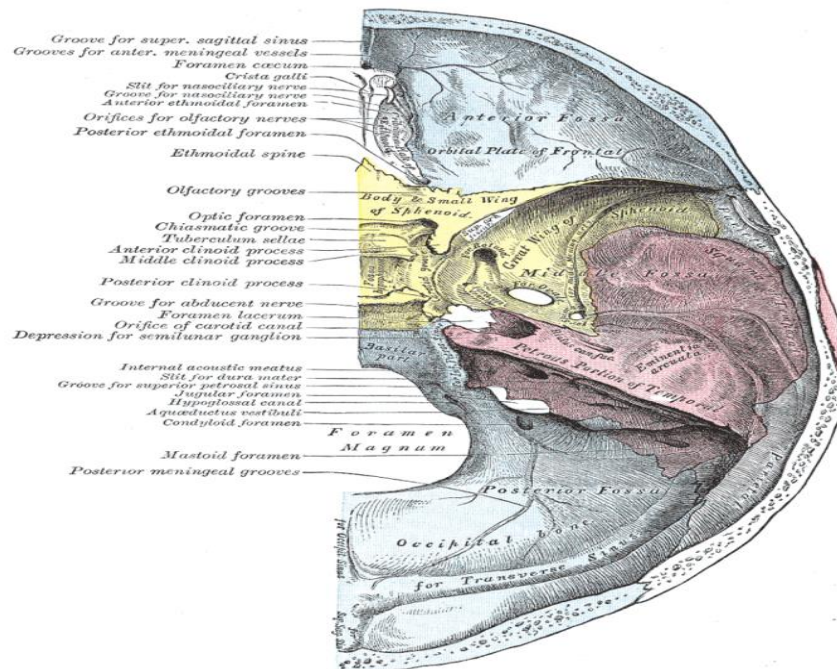


**Figure 2.3** shows foramina of the skull (Bontrager and Lampignano 2013)

### **2.1.2.8.1 Foramina in the skull includes:**

Supraorbital foramen, optic foramen, foramen magnum, foramina of cribriform plate and foramen rotundum.

### **2.1.2.9 Sutures:**

A suture is a type of fibrous joint (or synarthrosis) that only occurs in the skull (or cranium).

A suture is a type of fibrous joint (or synarthrosis) that only occurs in the skull. The bones are bound together by Sharpey's fibers, a matrix of connective tissue which provides a firm joint.

A small amount of movement is permitted through these sutures that contribute to the compliance and elasticity of the skull. The joint between the mandible and the cranium, known as the temporomandibular joint, forms the only non-sutured joint in the skull. Most sutures are named for the bones that they articulate.

At birth, many of the bones of the skull remain unfused to the soft spots described as fontanelle. The bones fuse relatively rapidly through a process known as craniosynostosis, although the relative positions of the bones can continue to change through life. In old age the cranial sutures may ossify completely, reducing the amount of elasticity present in the skull. As such, the degree of ossification can be a useful tool indetermining age postmortem(Bontrager and Lampignano 2013).

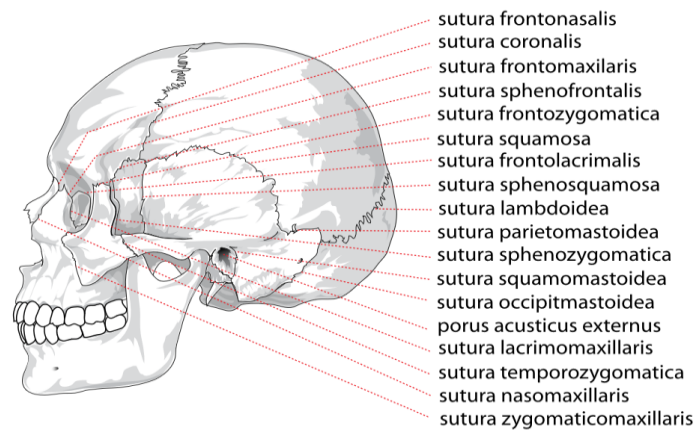


**Figure 2.4** Lateral view of a skull showing sutures (Bontrager and Lampignano 2013).

### 2.1.2.10 Paranasal Sinuses:

Paranasal sinuses are a group of four, paired, air-filled spaces that surround the nasal cavity (maxillary sinuses), above the eyes (frontal sinuses), between the eyes (ethmoid sinuses), and behind the eyes (sphenoid sinuses). The sinuses are named for the facial bones that they are located behind (Bontrager and Lampignano 2013).

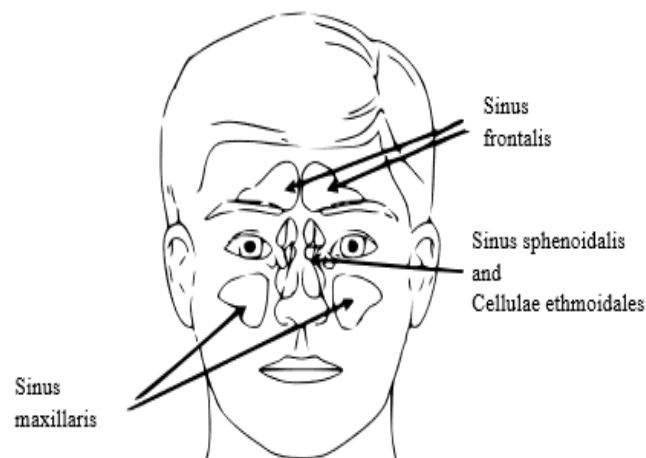


**Figure 2.5** shows sinuses (Bontrager and Lampignano 2013).



The maxillary sinuses (also called the maxillary antrechea, the largest of the paranasal sinuses) are located under the orbits in the maxillary bones(Bontrager and Lampignano 2013).

The frontal sinuses are superior to the orbits and are in the frontal bone.

The ethmoid sinuses are formed from several discrete air cells within the ethmoid bone between the nose and the orbits.

The sphenoid sinuses are in the sphenoid bone at the center of the skull base under the pituitary gland.

The paranasal sinuses are lined with respiratory epithelium.

The paranasal sinuses form developmentally through excavation of bone by air-filled sacs (pneumatic diverticula) from the nasal cavity. This process begins prenatally and continues through the course of an individual's lifetime(Bontrager and Lampignano 2013).

#### **2.1.2.10.1 Function of the Paranasal Sinuses:**

The biological role of the sinuses is debated, but a number of possible functions have been proposed. These include:

Decreasing the relative weight of the front of the skull, and especially the bones of the face, increasing resonance of the voice, providing a buffer against blows to the face, insulates sensitive structures like dental roots and eyes from rapid temperature fluctuations in the nasal cavity, humidifying and heating of inhaled air because of slow air turnover in this region, regulation of intranasal and serum gas pressures and immunological defense(Bontrager and Lampignano 2013).

## **2.2 Skull metastasis:**

Metastases to the skull are very common in patients with disseminated skeletal metastatic disease, although they are often asymptomatic (Greenberg, Deck et al. 1981).

### **2.2.1 Epidemiology:**

Skull metastases are seen in ~20% (range 15-25%) of all cancer patients. The demographics of patients with skull metastases will mirror those of the primary tumor, and as such in general they are found in the older population (Greenberg, Deck et al. 1981).

### **2.2.2 Clinical presentation:**

Although over half of all skeletal metastases are asymptomatic, they can cause symptoms in a number of scenarios (Greenberg, Deck et al. 1981).

Mass effect on adjacent structures:

Compression of brain/brainstem, focal neurological deficits, seizures, compression of exiting cranial nerves, compression/invasion/occlusion of dural venous sinuses and dural venous sinus thrombosis and proptosis.

Mechanical instability:

Occipital condyle compression fracture and temporomandibular joint instability (Greenberg, Deck et al. 1981).

### **2.2.3 Pathology:**

Primary tumors most frequently encountered as metastases to the skull include:

Breast cancer, lung cancer, Melanoma, Prostate cancer, Thyroid cancer (usually follicular), Renal cell cancer, Lymphoma, Leukemia, Multiple myeloma and Intrahepatic cholangiocarcinoma

In children both neuroblastoma (skull metastases are not infrequently the first sign of disease) and Ewing sarcoma are encountered (Greenberg, Deck et al. 1981).

#### **2.2.4 Radiographic features:**

Skull metastases have the same range of appearances as skeletal metastases elsewhere, and in 90% of cases other skeletal metastases are evident. Lytic metastases (most common) and sclerotic metastasis can particularly occur from breast and prostate cancers (Stark, Eichmann et al. 2003).

It is worth remembering that occasionally a solitary skull metastasis may be the only evidence of metastatic disease. This is particularly the case with renal cell carcinoma and thyroid carcinoma (Stark, Eichmann et al. 2003).

#### **2.2.5 Treatment and prognosis:**

For asymptomatic lesions, no specific treatment is required above or beyond systemic treatment being administered. Even when symptomatic, in many instances patients are being palliated and as such no focal therapy is instituted (Stark, Eichmann et al. 2003).

In instances where symptoms are significant and the general health and prognosis warrants intervention, a number of options exist:

##### **2.2.5.1 Radiotherapy:**

Whole brain radiotherapy if cerebral or leptomeningeal metastases are present or focal radiotherapy for single/symptomatic lesions (Stark, Eichmann et al. 2003).

### **2.2.5.2 Chemotherapy:**

Usually already instituted for systemic disease (Stark, Eichmann et al. 2003).

### **2.2.5.3 Surgery:**

Reserved for larger symptomatic lesions and has a role in diagnosis, when the lesion is solitary or diagnosis not established. It is difficult to say anything sensible when discussing prognosis, as clearly the degree of systemic disease, and the primary tumor and its response to therapy is going to have a huge impact. In general, it is safe to say however that in most instances, skeletal metastases represent advanced disease with poor prognosis, typically measured in weeks and months (Stark, Eichmann et al. 2003).

### **2.2.6 Bone Scan:**

The skeletal system serves as a framework to support the soft tissues of the body. In contrast to popular belief, the bone is a live functional tissue undergoing continuous metabolic changes. The bone serves as a storehouse for calcium and phosphorus, protects soft organs, and works as a lever for muscles. Bone tissues consist of organic and inorganic constituents, the organic matrix accounting for almost one third of the weight of the bone, and the inorganic matrix forming the rest. The inorganic matrix is called hydroxyapatite crystal and is primarily composed of calcium phosphate and, to a small extent, carbonate and hydroxide. Inorganic calcium salts deposit within the frame of the organic matrix and give strong rigidity to the bone. The blood supply is essential for the growth of new bone; a continuous exchange of minerals takes place between bone and plasma, and the minerals are used in new bone

formation. This process of mineral exchange and new bone formation, by which new bone gradually replaces old bone, is called bone accretion. A fracture repairs itself by new bone formation(Saha 2012).

**Radiopharmaceuticals and Imaging Techniques**  
**<sup>99m</sup>Tc-Phosphonate and Phosphate Complexes**  
The <sup>99m</sup>Tc complexes such as PYP, MDP, and HDP are the agents used for bone imaging. Several studies have shown superiority of one agent over another, but the general consensus is that <sup>99m</sup>Tc-MDP, and <sup>99m</sup>Tc-HDP exhibit essentially similar behavior in vivo, whereas <sup>99m</sup>Tc-PYP bone scans are somewhat inferior in quality. Currently, <sup>99m</sup>Tc-MDP is most commonly used for bone scanning. The plasma clearance half-time of these compounds is about 3 to 4 min, although it is slightly longer for <sup>99m</sup>Tc-PYP. The plasma protein binding of <sup>99m</sup>Tc-PYP is more than those of <sup>99m</sup>Tc-MDP and <sup>99m</sup>Tc-HDP by almost a factor of two; hence, there is a slower plasma clearance of the former. Urinary excretion of <sup>99m</sup>Tc-MDP is nearly 75% to 85% in 24 hr, whereas it is about 60% for <sup>99m</sup>Tc-PYP (Isawa 1998). The skeletal retention of <sup>99m</sup>Tc-HDP is about 50% of the injected dosage in 24 hr(Lorberboym, Macadziob et al. 2005). Approximately 10 to 20 mCi (370–740 MBq) <sup>99m</sup>Tc-MDP or <sup>99m</sup>Tc-HDP is injected intravenously and scanning is performed with the patient supine 2 to 3 hr after injection. The 2- to 3-hr waiting period is needed to reduce the background against the bone, and the patient is asked to void before imaging so that the bladder activity does not blur the pelvic region on the image. Whole-body scanning is performed by moving the detector from head to toe of the patient using either a single-head or a dual-head camera equipped with a low-energy, all-purpose parallel hole collimator. Static spot images are obtained with a single-head camera, whereas both anterior and posterior scans are obtained simultaneously using a dual head whole-body camera(Saha 2012).

Regional bone blood flow rate, bone formation rate, and extraction efficiency are the major factors that influence the bone uptake of phosphonate complexes. In general, the higher the rates of blood flow and bone formation, the greater the bone uptake of radiotracer. There are two hypotheses on the bone uptake mechanism of phosphonate compounds: hydroxyapatite uptake and collagen uptake. In the hydroxyapatite uptake theory, it has been suggested that hydroxyapatite crystal removes the phosphonate component successfully from  $^{99m}\text{Tc}$ -phosphate complexes, thus setting the reduced technetium free to bind independently to hydroxyapatite at another binding site. In the collagen uptake theory, it has been suggested that  $^{99m}\text{Tc}$ phosphonate complexes localize in both inorganic and organic matrices of bone, the latter uptake depending on the amount of immature collagen present. It has also been found that  $^{99m}\text{Tc}$ -phosphonate complexes localize in soft tissues and tumors to a variable degree (Saha 2012).

### **2.2.7 Diagnosis:**

Various diseases that are diagnosed by increased uptake of  $^{99m}\text{Tc}$ -phosphonate compounds include metastatic lesion, Paget's disease, fracture, osteomyelitis, bone tumor, rheumatoid arthritis, and any other disorder that results in active bone formation (Saha 2012).

### **2.2.8 Types of Bone Scan:**

Dynamic bone scans and Static bone scans.

#### **2.2.8.1 Dynamic bone scans:**

##### **2.2.8.1.1 Indications:**

Differentiation between Osteomyelitis and cellulites, Detection and evaluation of infections and Avascular necrosis.

## **2.2.8.2 Static Bone Scan:**

### **2.2.8.2.1 Indications:**

Bone metastases (benign or malignant tumors), Bone trauma, Osteomyelitis, Lower back pain, Stress fracture, Osteosarcoma and Multiple myeloma.

### **2.2.8.2.2 Contraindication:**

Patient who has recently ingested contrast media for different study and Patient who has recently (24-48) hours had a technetium based nuclear medicine scan.

## **2.2.9 Indications for Bone SPECT:**

In areas of complex anatomy (substantial superimposition of bony structures) bone SPECT is necessary (Roos, van Isselt et al. 1987).

Generally done in areas such as: Lumbar spine, Temporomandibular joints (TMJ)/skull, Hip / Sacro-iliac joint and Knee (Saha 2012).

## **2.2.10 Normal Scan:**

Symmetrical and Uniform uptake with increased activity in Joints, junctions, and scapulas.

Nasopharynx and soft tissue uptake, Kidneys show lightly and bladder shows brightly.

Liver uptake can be a normal variant if there is slow release or liver disease. Older patients may have a globally poor quality scan (Saha 2012).

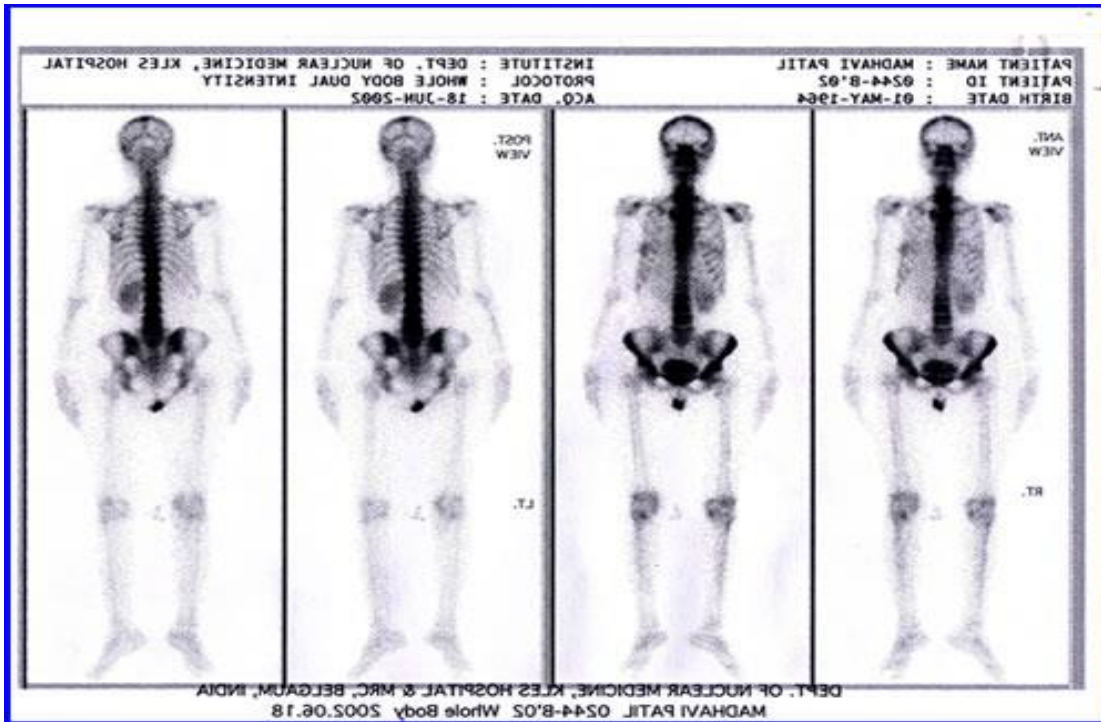


**Figure2.6** Shows normal bone scan(Bisson, Vickers et al. 1974).

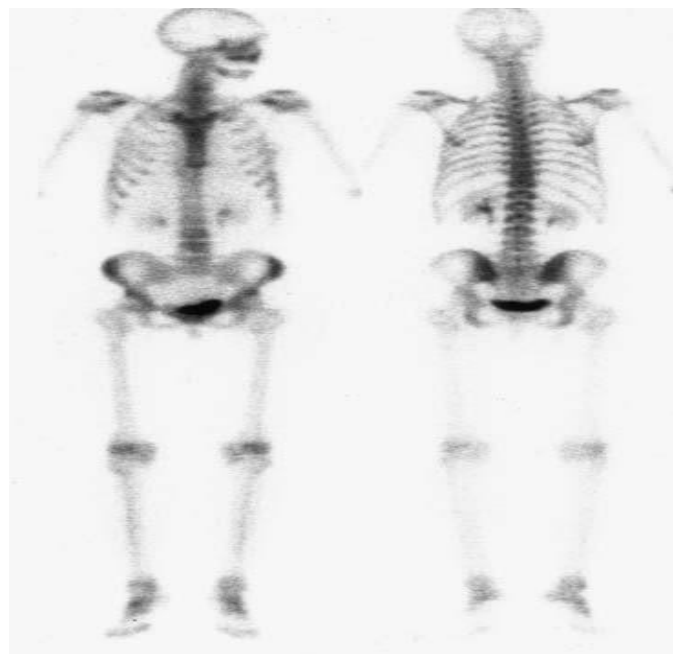


**Figure2.7** shows normal adult bone scan(Bisson, Vickers et al. 1974).



### 2.2.11 Abnormal Scan:

Abnormal uptake may appear as focal area of increased or decreased activity. Bone uptakes showing brightly, no kidney or bladder.

Cold lesions: Diminished activity or none is indicative of osteonecrosis, osteoporosis, osteomalacia, multiple myeloma, radiation therapy, end-stage cancer patients, renal cell carcinoma, thyroid cancer, anaplastic tumors, neuroblastoma.

Osteomyelitis appears as increased uptake in flow, blood pool, and delays. While Cellulitis appears as increased uptake in flow and blood pool with mild or no uptake in delays.

Prosthesis loosening and infection appears as increased activity around prosthesis on bone surfaces and inside bone surfaces.

Primary malignant tumors (osteogenic and chondrosarcomas) increased vascular flow, blood pool, and delays focally

Benign primary tumors (osteoid, osteoma) increased blood pool and delays, focally intense (Saha 2012).

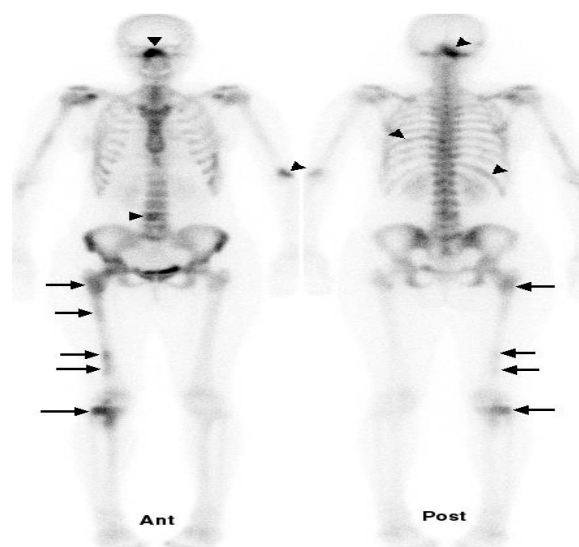


**Figure 2.8** shows abnormal bone scan (Bisson, Vickers et al. 1974).

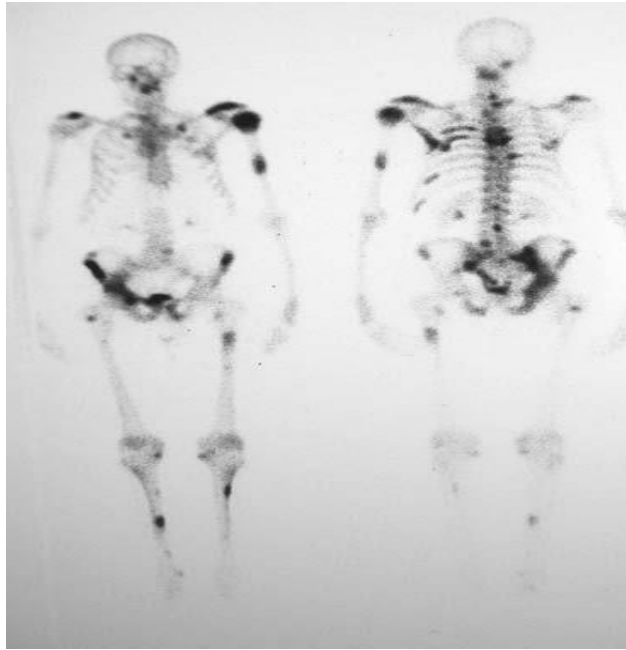


**Figure 2.9** shows a widespread skeletal metastases prostate (Bisson, Vickers et al. 1974).

## **2.3 Instruments for Radiation Detection and Measurement:**

In nuclear medicine, it is necessary to ascertain the presence, type, intensity, and energy of radiations emitted by radionuclides, and these are accomplished by radiation-detecting instruments. The two commonly used devices are gas-filled detectors and scintillation detectors with associated electronics (Saha 2012).

### **2.3.1 Gas Filled Detectors:**

The operation of a gas-filled detector is based on the ionization of gas molecules by radiations, followed by collection of the ion pairs as current with the application of a voltage between two electrodes. The measured current is primarily proportional to the applied voltage and the amount of radiations. The two most commonly used gas-filled detectors are ionization chambers and Geiger-Müller (GM) counters. The primary difference between the two devices lies in the operating voltage that is applied between the two electrodes. Ionization chambers are operated at 50–300

V, whereas the GM counters are operated at around 1000 V(Saha 2012) (Saha GB,et al.2006).Examples of ionization chambers are “CutiePie” counters and dose calibrators, which are used for measuring high intensity radiation sources, such as output from x-ray machines (Cutie-Pie) and activity of radiopharmaceuticals (dose calibrators). The GM counters are used for detecting low-level beta and gamma radiations(Roos, van Isselt et al. 1987).

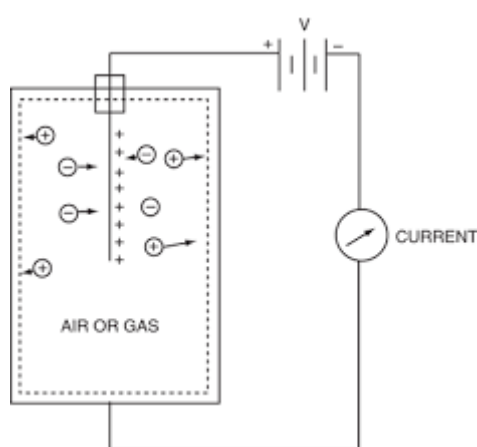


**Figure2.10**Schematic diagram of a gas filled detector(Lansiart, Morucci et al. 1966).

### 2.3.2 Scintillation Detecting Instruments:

A variety of scintillation or g-ray detecting equipment is currently used in nuclear medicine. All these instruments are g-ray detecting devices and consist of a collimator (excluding well counter), sodium iodide detector, photomultiplier tube, preamplifier, pulse height analyzer, X, Y positioning circuit (only in scintillation cameras), and display or storage(Saha 2012). Basically, g rays from a source interact in the sodium iodide detector and light photons are emitted. The latter strike the photocathode of a photomultiplier (PM) tube and a pulse is generated at the end of the PM tube. The pulse is first amplified by a preamplifier and then by a linear amplifier. A pulse height analyzer sorts out the amplified

pulses according to the desired energy of the  $\gamma$  ray and finally feeds the pulse into a scaler, magnetic tape, computer, cathode ray tube, or x-ray film(Saha 2012).

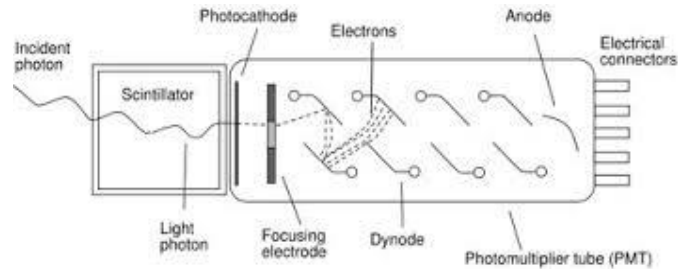


**Figure 2.11** Schematic diagram of a scintillation detector(Suga, Clark et al. 1961).

### 2.3.2.1 Collimator:

In all nuclear medicine equipment for imaging, a collimator is attached to the face of a sodium iodide detector to limit the field of view so that all radiations from outside the field of view are prevented from reaching the detector. Collimators are made of lead and have a number of holes of different shapes and sizes. In scintillation cameras, collimators are classified as parallel hole, diverging, pinhole, and converging, depending on the type of focusing (Saha 2012).

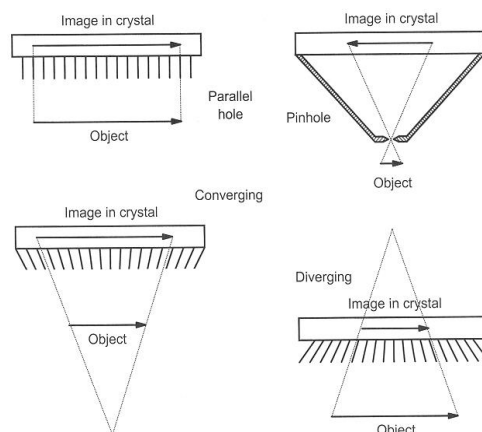


**Figure 2.12** Shows different types of collimators (Roos, van Isselt et al. 1987).

### **2.3.2.2 Photocathode:**

This converts light into electrons (Saha 2012) (Saha GB,et al.2006).

### **2.3.2.3 Photomultiplier tubes:**

A PM tube consists of a light-sensitive photocathode at one end, a series (usually 10) of metallic electrodes called dynodes in the middle, and an anode at the other end—all enclosed in a vacuum glass tube. The PM tube is fixed on to the NaI(Tl) crystal with the photocathode facing the crystal with a special optical grease. The number of PM tubes in the thyroid probe and the well counter is one, whereas in scintillation cameras it varies from 19 to 94 which are attached on the back face of the NaI(Tl) crystal. A high voltage of ~1000 V is applied from the photocathode to the anode of the PM tube in steps of ~100 V between dynodes. When a light photon from the NaI(Tl) crystal strikes the photocathode, photoelectrons are emitted, which are accelerated toward the immediate dynode by the voltage difference between the electrodes. The accelerated electrons strike the dynode and more secondary electrons are emitted, which are further accelerated. The process of multiplication of secondary electrons continues until the last dynode is reached, where a pulse of  $10^5$ – $10^8$  electrons is produced. The pulse is then attracted to the anode and finally delivered to the preamplifier(Saha 2012).

### **2.3.2.4 Preamplifier:**

The pulse from the PM tube is small in amplitude and must be amplified before further processing. It is initially amplified with a preamplifier that is connected to the PM tube. A preamplifier is needed to adjust the voltage of the pulse shape and match the impedance levels between the

detector and subsequent components so that the pulse is appropriately processed by the system (Saha 2012).

### **2.3.2.5 Linear Amplifier**

The output pulse from the preamplifier is further amplified and properly shaped by a linear amplifier. The amplified pulse is then delivered to a pulse height analyzer for analysis as to its voltage. The amplification of the pulse is defined by the amplifier gain given by the ratio of the amplitude of the outgoing pulse to that of the incoming pulse, and the gain can be adjusted in the range of 1–1,000 by gain controls provided on the amplifier. The amplitudes of output pulses normally are of the order of 0–10 V (Saha 2012).

### **2.3.2.6 Pulse Height Analyzer:**

Gamma rays of different energies can arise from a source, either from the same radionuclide or from different radionuclides, or due to scattering of g-rays in the source. The pulses coming out of the amplifier may then be different in amplitude due to differing g-ray energies. The pulse height analyzer (PHA) is a device that selects for counting only those pulses falling within preselected voltage amplitude intervals or “channels” and rejects all others. This selection of pulses is made by control knobs, called the lower level and upper level, or the base and window, provided on the PHA. Proper choice of settings of these knobs determines the range of g-ray energies that will be accepted for further processing such as recording, counting, and so on. In scintillation cameras, these two knobs are normally replaced by a peak voltage control and a percent window control. The peak voltage control relates to the desired g-ray energy and the percent window control indicates the window width in percentage of the desired g-ray energy, which is set symmetrically on each side of the peak voltage. A pulse height analyzer normally selects only one range of

pulses and is called a single-channel analyzer (SCA). A multichannel analyzer (MCA) is a device that can simultaneously sort out pulses of different energies into a number of channels. By using an MCA, one can obtain simultaneously a spectrum of  $\gamma$  rays of different energies arising from a source (Saha 2012).

### **2.3.2.7 Display or Storage**

Information processed by the PHA is normally given in the form of pulses and counts that are stored for further processing. Counts can be recorded for preset counts or time. In thyroid probes and well counters, counts are displayed on a scalar, whereas in scintillation cameras, these counts are stored in a computer and processed further to form images (Saha 2012).

## **2.4 Single Photon Emission Computed Tomography:**

The most common SPECT systems consist of a typical gamma camera with one to three NaI(Tl) detector heads mounted on a gantry, an on-line computer for acquisition and processing of data and a display system. The detector head rotates around the long axis of the patient at small angle increments (3–10) degree for 180 or 360 angular sampling.

The data are stored in a 64 x 64 or 128 x 128 matrix in the computer for later reconstruction of the images of the planes (slices) of interest. Transverse, sagittal, and coronal images can be obtained from the collected data (Saha 2012).



**Figure 2.13** Shows SPECT camera (Rousso, Ziv et al. 2010).

## **2.5 Literature Review:**

**Sadeghi, Zakavi et al. (2008)** Their research was Age-related changes in skull uptake on bone scintigraphy (A quantitative study). "Hot skull, or diffuse, increased activity of bone seeking radiotracers, is frequently seen in the bone scans of some patients, especially elderly women". This finding has been attributed to enhanced bone metabolism in old age. The skull to femoral ratio was significantly higher in female patients in the age groups 30-39 and above. In females, the five upper age groups (30-39, 40-49, 50-59, 60-69, and 70 and above) had significantly higher SFR than the lower age groups. In males, the two upper age groups (60-69, 70 and above) had significantly higher SFR than the lower age groups. The findings in males were not concordant with the previous studies addressing this issue, which could be explained by different bone mineral density in the Iranian population. Their data showed that "hot skull" is not necessarily an abnormal finding, especially in elderly women.



**Lorberboym, Macadziob et al. (2005).** We have frequently observed diffusely increased skull activity on bone scans of obese patients, who do not have evidence of metabolic or metastatic bone disease. Skull activity of 25 obese patients was compared to that of age and sex matched non obese 25 patients visually and quantitatively. The results clearly indicated that diffusely increased skull activity is significantly more common on bone scans of obese patients because of disparate attenuation of overlying soft tissues.

**Suematsu, Yoshida et al. (1992).** Diffusely increased skull uptake (a hot skull) is often seen in patients with bone metastases and metabolic diseases. This finding is also, however, noticed in normal bone scans of aged women. To determine whether the hot skull could be considered a normal variant in elderly women and is associated to menopause, we studied 282 normal bone scans (166 women and 116 men without metabolic and hormonal disease; age range 11 to 84 yr). The sex dependent difference in skull uptake began to develop in the age group 30-39 yrs (p less than 0.05). The skull showed greater activity in women than in men for age groups from 30-39 to 80-89 yrs. In the age groups 50-59 and 60-69, the difference was particularly large (p less than 0.001).

**Roos, van Isselt et al. (1987).** Diffusely increased uptake in the calvarium on bone scintigraphy (a hot skull) is often present in patients with bone metastases and metabolic diseases. Excluding these known facts the prevalence of the hot skull and its relation with malignancy and, more specifically, with breast carcinoma have been studied in 673 patients. In women, the hot skull is clearly related to malignancy and to lesser extent to breast carcinoma. However, another remarkable feature of the hot skull is its predominance in women in

general (compared to men) and, therefore, the data suggest that the hot skull can also represent a normal variant of female skull. They conclude that hot skull has no clinical value in screening protocol.

(Senda and Itoh 1987)The present study was undertaken to evaluate the finding of diffusely high uptake by the calvaria in a series of 994 consecutive whole body scans in regard to the incidence and degree, and to discuss the mechanism. Positive rate of the finding was 8.7% in total, 14.9% in women, and 2.6% in men. The difference between women and men was significant (P less than 0.001). The finding was significantly correlative with the ages of patients. On the basis of these results, the finding may be not only a side effect of intensive cytotoxic medication on the skeleton, but also a physiological event relative to bone change with age and postmenopausal osteoporosis.

## **Chapter Three**

### **Material and Method**

#### **3.1 Material:**

##### **3.1.1 SPECT Camera:**

Medical Imaging System (Mediso) was used for imaging. The manufacturer is Mediso Ltd. H-1022. The unit of processing used was Nucline (SN=ME0064914). 100-250V/50-60HZ. Made in Hungary. Whole-body scanning is performed by moving the detector from head to toe of the patient using either a single-head or dual-head camera equipped with a low-energy all-purpose parallel hole collimator (N-GK310000-0003V).



**Figure 3.1** SPECT camera used in this thesis

##### **3.1.2 Procedure:**

All patients underwent whole-body bone scan 2:30- 3 hours after intravenous injection of (phosphonomethyl) phosphonic acid-[<sup>99m</sup>Tc] technetium ([<sup>99m</sup>Tc]-MDP). Scanning is performed with the patient supine using knee support for patient comfort. Regions of interest (ROIs) were drawn on the anterior and posterior views of both skull and the average counts of each ROI were recorded.

Patients divided to 8 age groups: 20-30, 30-40, 40-50, 50-60, 60-70, 70-80, 80-90, 90 and above.

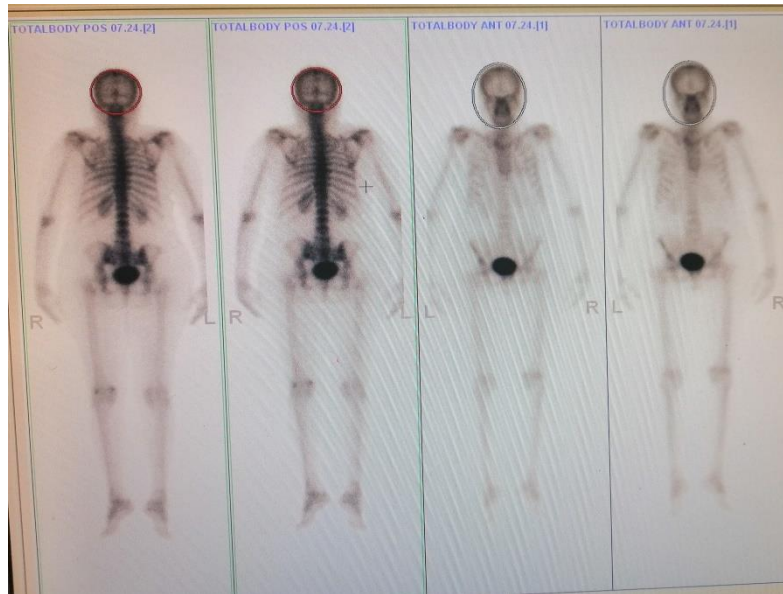


**Figure 3.2** Example of ROI (region of interest) drawing on the skull.

### **3.2 Method:**

#### **3.2.1 Study Design:**

This study is descriptive case control study.

#### **3.2.2 Area of study:**

This study conducted at Radiation and Isotope Center of Khartoum.

#### **3.2.3 Duration of Study:**

This study conducted in period from March 2019 until August 2019.

#### **3.2.4 Population of the study:**

##### **3.2.4.1 Inclusion criteria:**

The population of this study was data set (normal static bone Images), with patient of breast and prostate cancer. The study include both gender with their age ranged from 20 years to 100years old.

### **3.2.4.2 Exclusion criteria:**

All patients with dynamic bone Scintigraphy. This study was excluding all metastatic skull patients less than 20 years old and patients whose above 100 years old.

### **3.2.5 Sample size:**

This study was applied on 100 patients whose came to nuclear medicine department for bone Scintigraphy.

### **3.2.6 Ethical consideration:**

A permission letter from the head of the nuclear medicine departments of radiation and Isotope Center of Khartoum was taken for the collection of the data.

Patients' permission was taken before conducting the study and patients' names was anonymous.

### **3.2.7 Data Analysis and Presentation:**

The data was collected from nuclear medicine images using data collection sheet which was prepared specially for this task.

Data was analyzed by using Microsoft excel and Statistical Package for the Social Sciences SPSS software (version 25). Independent sample t-test was done for comparison of mean values between two independent groups. Cross tabulation between average count and gender was done.

P values less than 0.05 were considered statistically significant .

## Chapter Four

### Results

The research involved hundred patients on bone Scintigraphy (39 male and 61 female), the results of this study are provided below:

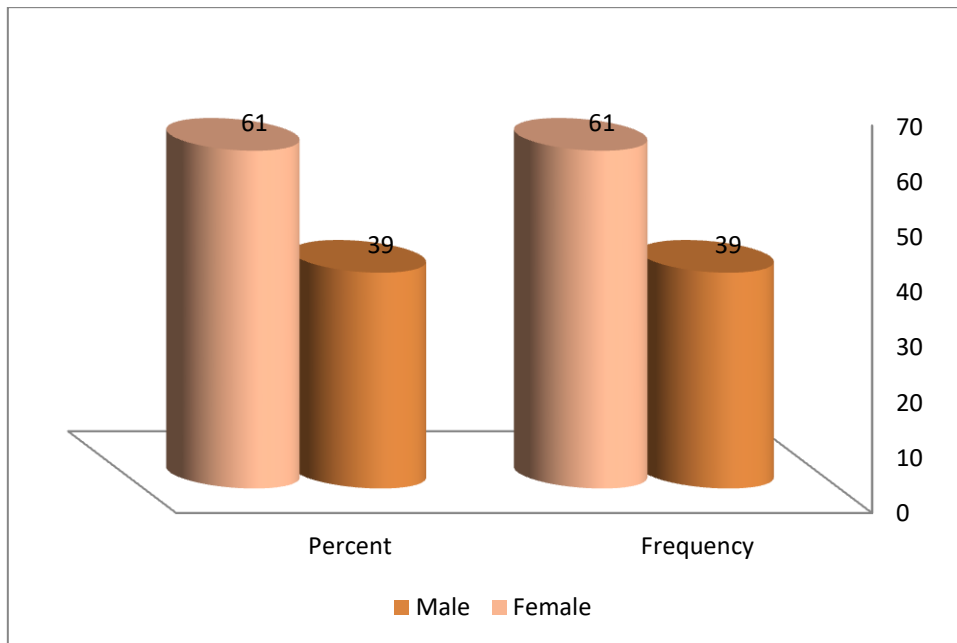


**Figure4.1** Bar chart shows the distribution of patients according to the gender.

**Table 4.1** shows the frequency of patients according to age groups

Age groups	Frequency	Percent
<30Y	4	4.0
<40Y	12	12.0
<50Y	19	19.0
<60Y	26	26.0
<70Y	21	21.0
<80Y	14	14.0
<90Y	4	4.0
Total	100	100

**Table 4.2** represent the frequency of skull uptake versus the body mass index among the sample population

Skull uptake	BMI	Frequency	Percent
Normal	under weight	2	3.7
	Normal	24	44.4
	Over weight	19	35.2
	Obesity	9	16.7
	Total	54	100
High	under weight	5	10.9
	Normal	23	50
	Over weight	8	17.4
	Obesity	10	21.7
	Total	46	100

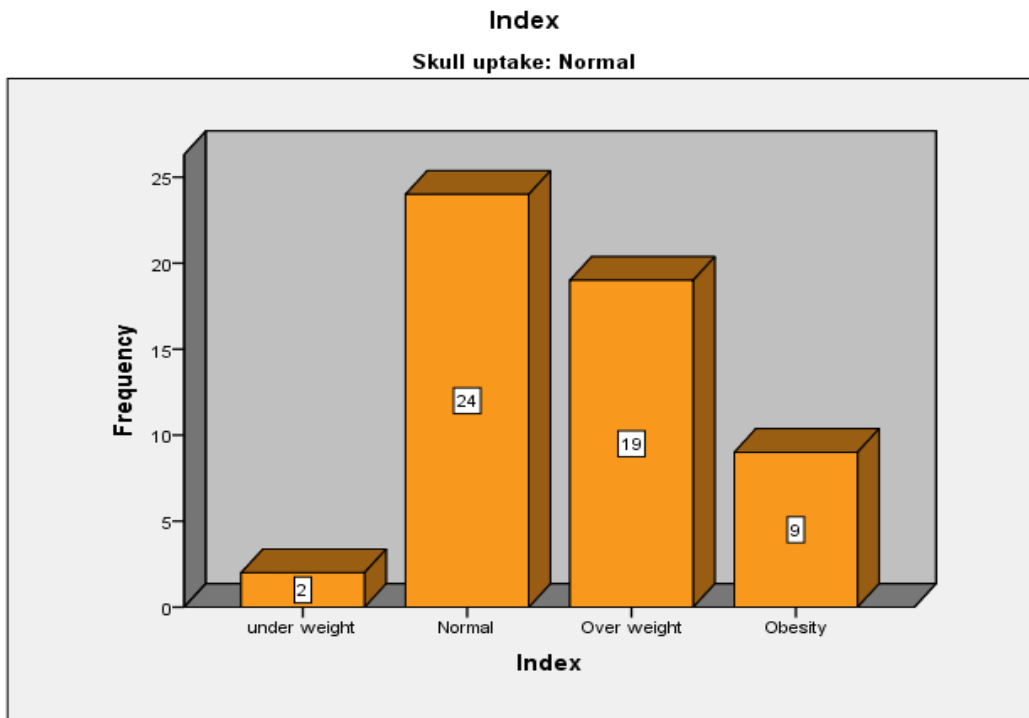


**Figure 4.2** histogram represents the frequency of normal skull uptake in different BMI.

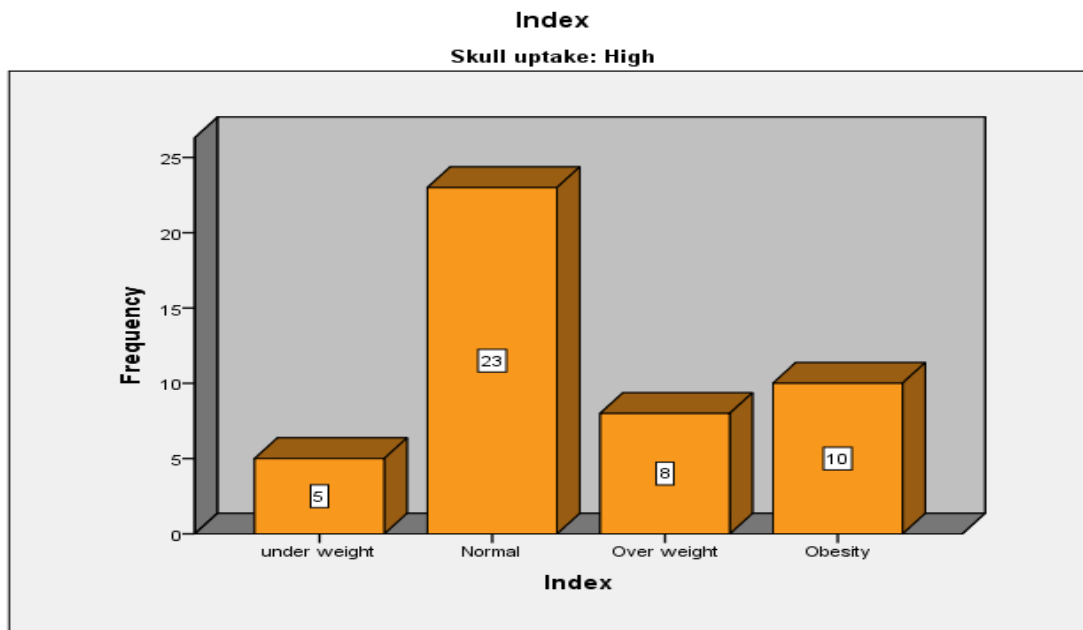


**Figure 4.3** histogram represents the frequency of abnormal skull uptake in different BMI.

**Table 4.3** shows crosstabulation of gender and age groups.

<b>Gender*Age groups crosstabulation</b>										
<b>Skull uptake</b>		<b>Age groups</b>	<b>&lt;30Y</b>	<b>&lt;40Y</b>	<b>&lt;50Y</b>	<b>&lt;60Y</b>	<b>&lt;70Y</b>	<b>&lt;80Y</b>	<b>&lt;90Y</b>	<b>Total</b>
Normal	Gender	Male	1	0	2	4	9	8	4	28
		Female	0	5	8	11	1	1	0	26
High	Gender	Male	1	0	0	3	4	3	0	11
		Female	2	7	9	8	7	2	0	35



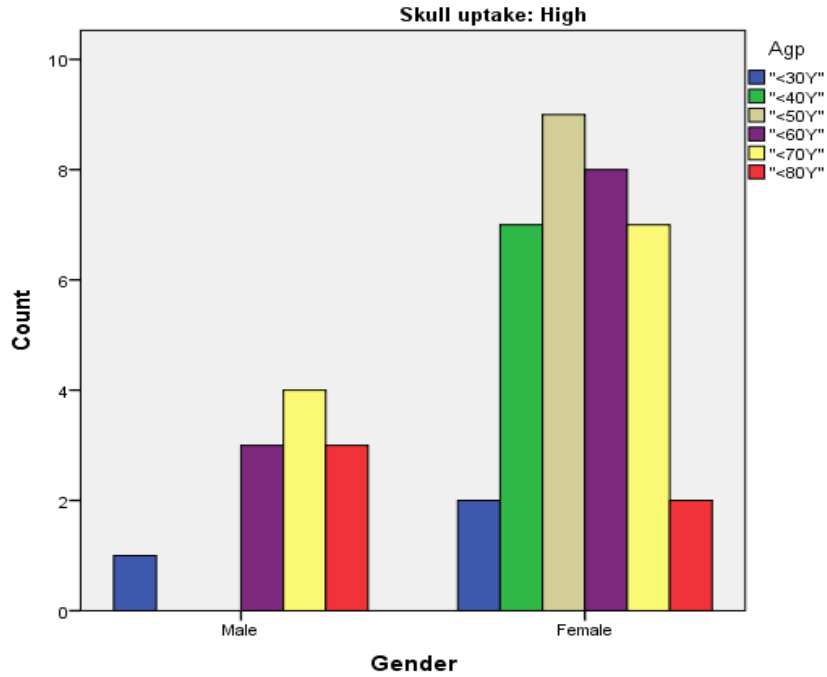


**Figure 4.4** histogram shows relationships between abnormal skull uptake, among gender and age groups.

**Table 4.4** shows the correlations between skull uptake and gender.

Correlations			
		Skull uptake	Gender
Skull uptake	Pearson Correlation	1	.285**
Sig. (2-tailed)			0.004
N		100	100
Gender	Pearson Correlation	.285**	1
Sig. (2-tailed)			0.004
N		100	100

\*\* Correlation is significant at the 0.01 level (2-tailed).

**Table 4.5** shows correlation between Age groups and average uptake.

Correlations				
			Age group	Average
Spearman's rho	Age group	Correlation Coefficient	1	-.316-**
		Sig. (2-tailed)	.	0.001
		N	100	100
	Average	Correlation Coefficient	-.316-**	1
		Sig. (2-tailed)	0.001	.
		N	100	100
** Correlation is significant at the 0.01 level (2-tailed).				

**Table 4.6** shows the frequency of skull uptake according to the disease.

Skull uptake		Disease	Frequency	Percent%
Normal	Valid	Ca breast	26	48.1
		Ca prostate	28	51.9
		Total	54	100
High	Valid	Ca breast	35	76.1
		Ca prostate	11	23.9
		Total	46	100

## Chapter Five

### Discussion, Conclusion and Recommendations

#### 5.1 Discussion:

Figure 4.1 shows the frequency of gender among sample population of 100 patients, which showed that a 39 male patients, while 61 female patients. While Table 4.1 showed the frequency of age groups among the population sample of 100 patients which showed a 26 of patients were <60Y, while 4 patients were <30Y.

Table 4.2 represent the frequency of skull uptake versus the body mass index among the sample population, Which showed a 54 of patients with normal skull uptake , while a 46 patients with high skull uptake. The obese and over weight patients represent (16.7- 35.2%) with normaluptake and (21.7-17.4%) with high uptake respectively. This study agreed with (Lorberboym, Macadziob et al. (2005),that increased activity in obese and over weight patients.

Table 4.3 represents the relationship between the skull uptake, gender and age groups among the study population. The skull uptake was significantly higher in female patients in the age groups 30-39 and above. While in males the upper age groups (60-69, 70 and above) had significantly higher uptake than the lower age group. This study agreed with (Sadeghi, Zakavi et al. 2008) at this part. Whereas 35 of female patients had higher uptake levels compare to 11 male patients, which agreed with (Suematsu, Yoshida et al. 1992).

Table 4.4 shows a Pearson correlation was run to determine the relationship between skull uptake and gender and was result in strong a significant correlation between them as shown in P-value relation:

(( $r=.258$ ,  $n=100$ ,  $p<0.01$ )). This study agreed with (Susematsu ,et al. 1992).

Table 4.5 ASpearman's rho was run to determine correlation between age and average uptake among population study. There was significant correlation between them (( $r= -.316$ ,  $n=100$ ,  $p<0.001$ )). This study agreed with (Senda K,et al,1987).

Table 4.6 showed frequency of skull uptake according to the disease among study population of 100 patients. This showed 26 Ca-breast patients had normal uptake, while 28 Ca-prostate patients had normal uptake. Also it showed that 35 Ca breast patients had high skull uptake, while 11 Ca prostate had high skull uptake. This study agreed with (Roos, van Isselt et al. 1987).

## **5.2 Conclusion:**

The research concluded that (hot skull), is not necessary an abnormal finding, especially in elderly women. There is significant correlation between age and skull uptake. On the basis of these results, the finding may be not only a side effect of intensive cytotoxic medication on the skeleton, but also a physiological event relative to bone change with age and postmenopausal osteoporosis.

The researcher observes the diffusely increased uptake on bone Scintigraphy of obese patients who don't have evidence of metastatic or metabolic disease because of disparate attenuation of overlying soft tissues.

In women, the hot skull is clearly related to malignancy and to lesser extent to breast carcinoma. However, another remarkable feature of the hot skull is its predominance in women in general (compared to men) and, therefore, the data suggest that the hot skull can also

represent a normal variant of female skull. We conclude that hot skull has no clinical value in screening protocol.

### **5.3 Recommendations:**

- Researcher recommends that every nuclear medicine department uses its own normal values and reference samples for quantitative evaluation. Socio-economic and racial variations between different patient populations should be considered when reporting bone scans.
- Using the normal values and references from other institutions (especially when located in countries with different cultural and socio-economic background) can cause interpretation mistakes and should be avoided if possible.
- A large sample size is needed for further confirmation.

## References

- Bisson, J., et al. (1974). "Bone scan: in clinical perspective." The Journal of urology 111(5): 665-669.
- Bontrager, K. L. and J. Lampignano (2013). Textbook of radiographic positioning and related Anatomy-E-Book, Elsevier Health Sciences.
- Greenberg, H. S., et al. (1981). "Metastasis to the base of the skull clinical findings in 43 patients." Neurology 31(5): 530-530.
- Isawa, T. (1998). Radiopharmaceuticals and Imaging Techniques. Nuclear Imaging of the Chest, Springer: 31-62.
- Kakhki, V. D. and S. R. Zakavi (2006). "Age-related normal variants of sternal uptake on bone scintigraphy." Clinical nuclear medicine 31(2): 63-67.
- Kigami, Y., et al. (1996). "Age-related change of technetium-99m-HMDP distribution in the skeleton." Journal of Nuclear Medicine 37(5): 815-818.
- Lam, M., et al. (2007). "Bone seeking radiopharmaceuticals for palliation of pain in cancer patients with osseous metastases." Anti-Cancer Agents in Medicinal Chemistry (Formerly Current Medicinal Chemistry-Anti-Cancer Agents) 7(4): 381-397.

- Lansiart, A., et al. (1966). "Gas-filled avalanche or spark producing image intensifier detector for X and  $\gamma$  rays." IEEE Transactions on Nuclear Science 13(3): 393-398.
- Lorberboym, M., et al. (2005). "The hot skull sign on bone scans of obese patients resulting from disparate soft tissue attenuation." Clinical nuclear medicine 30(10): 680-681.
- Pour, M. C., et al. (2004). Diffuse increased uptake on bone scan: super scan. Seminars in nuclear medicine, WB Saunders.
- Roos, J. C., et al. (1987). "The hot skull: malignant or feminine?" European journal of nuclear medicine 13(4): 207-209.
- Rousso, B., et al. (2010). Dynamic SPECT camera, Google Patents.
- Ryan, P. and I. Fogelman (1997). Bone scintigraphy in metabolic bone disease. Seminars in nuclear medicine, Elsevier.
- Sadeghi, R., et al. (2008). "Age-related changes in skull uptake on bone scintigraphy: a quantitative study." Nuclear Medicine Review 11(2): 67-69.
- Saeed, I. E., et al. (2014). "Cancer incidence in Khartoum, Sudan: first results from the Cancer Registry, 2009–2010." Cancer medicine 3(4): 1075-1084.

Saha, G. B. (2012). Physics and radiobiology of nuclear medicine, Springer Science & Business Media.

Senda, K. and S. Itoh (1987). "Evaluation of diffusely high uptake by the calvaria in bone scintigraphy." Annals of nuclear medicine 1(1): 23-26.

Stark, A. M., et al. (2003). "Skull metastases: clinical features, differential diagnosis, and review of the literature." Surgical neurology 60(3): 219-225.

Suematsu, T., et al. (1992). "Diffusely increased uptake in the skull in normal bone scans." Kaku igaku. The Japanese journal of nuclear medicine 29(5): 599-605.

Suga, K., et al. (1961). "Scintillation Detector of 4-m<sup>2</sup> Area and Transistorized Amplifier with Logarithmic Response." Review of Scientific Instruments 32(11): 1187-1189.



# Appendices

Sudan university of Science and Technology

Faculty of Graduate Studies

Ms.c Nuclear Medicine

## Evaluation of Diffusely High Uptake of Skull in Breast and Prostate Cancer using Bone Scintigraphy

### Appendix (1)

#### Data Collection Sheet

1-Patient No	<input type="text"/>
2- Age	<input type="text"/> rs old
3-Gender	<input type="text"/> Male <input type="text"/> Female
4-Weight	<input type="text"/>
5-Height	<input type="text"/> Cm
6-Dose	<input type="text"/>
7- Radiopharmaceutical	<input type="text"/>
8-No of Total Counts	<input type="text"/> count
9- No of Anterior Skull Counts	<input type="text"/> count
10- No of Posterior Skull Counts	<input type="text"/> count
11- Average Skull Counts	<input type="text"/> count
12-Skull Counts	<input type="text"/> Normal <input type="text"/> High
13-Patient Disease	<input type="text"/>